Conical Diffraction and Gap Solitons in Honeycomb Photonic Lattices

Or Peleg,[1] Guy Bartal,[1] Barak Freedman,[1] Ofer Manela,[1] Mordechai Segev,[1] and Demetrios N. Christodoulides[2]

[1]*Department of Physics and Solid State Institute, Technion, Haifa 32000, Israel*

[2]*College of Optics & Photonics–CREOL, University of Central Florida, Orlando, Florida 32816, USA*

(Received 15 August 2006; published 6 March 2007)

We study wave dynamics in honeycomb photonic lattices, and demonstrate the unique phenomenon of conical diffraction around the singular diabolical (zero-effective-mass) points connecting the first and second bands. This constitutes the prediction and first experimental observation of conical diffraction arising solely from a periodic potential. It is also the first study on k space singularities in photonic lattices. In addition, we demonstrate ''honeycomb gap solitons'' residing in the gap between the second and the third bands, reflecting the special properties of these lattices.

DOI: 10.1103/PhysRevLett.98.103901 PACS numbers: 42.70.Qs

Most often, the dynamics of a linear physical system can be described by its dispersion relation. In some systems, two equal-energy surfaces intersect at a single, special point: the diabolic point [1]. The diabolic point is a singular point, for which the direction of the group velocity is not uniquely defined. Such a dispersion surface appears in a two-dimensional honeycomb lattices [2] (see Fig. 1), as recently demonstrated in graphene [3]. Graphene, a monolayer of graphite for which the atoms are packed in a honeycomb structure, displays intriguing features, such as extremely high electron mobility [3]. The electrons around the diabolical points of the band structure in graphene behave as ''massless fermions'' as a result of the linear slope around the diabolical points. The concept of diabolical points arising from the intersection of two dispersion curves have been expanded to other realities, e.g., level-crossing in quantum mechanics [4], magnetic molecules [5], quantum chemistry [6], etc.

In optics, diabolical points were first discovered by Hamilton [7], who predicted that a collimated randomly polarized ray of light entering a biaxial crystal in the direction of the diabolical point, will undergo refraction into a cone of light. This phenomenon was named conical diffraction [7]. It was observed by Lloyd [8] and was intensively studied since then [1,9]. The physical origin of Hamilton's conical diffraction, and in all experiments on conical diffraction ever since, was a singularity in k space due to polarization. That is, all published work on conical diffraction deals with k space singularities due to polarization. However, as noted above, diabolical points also exist in the band structure of the honeycomb lattice, where their origin is the special symmetry of the lattice. Hence, it is natural to ask, can diabolic points in a honeycomb lattice give rise to conical diffraction effects? If so, then conical diffraction in honeycomb lattices would arise from completely different physical origins than ''traditional'' conical diffraction effects do: conical diffraction in a honeycomb lattice will arise solely from the symmetry of the structure.

Here we study the dynamics of optical waves in honeycomb photonic lattices. We show that the band-crossing points are diabolic points, about which conical diffraction occurs [10]. We demonstrate that an incident narrow light beam, with momentum at the vicinity of a diabolic point, diffracts in the lattice [11] in a characteristic conical form, attaining the shape of a ring whose thickness does not broaden, whereas its radius grows linearly with distance. This constitutes the first prediction and experimental observation of conical diffraction arising solely from the periodicity of a potential, with no birefringence effects involved. This study is also the first to explore k space singularities in photonic lattices. To illustrate the special features of the honeycomb lattice, we also demonstrate spatial gap solitons in honeycomb lattices.

The ideas presented here are universal for any honeycomb lattice. However, for concreteness, we consider the specific case of our experiments, which are carried out in a photonic lattice constructed by optical induction [12–14]. The honeycomb lattice [Fig. 1(a)] can be represented as a two atom basis with a hexagonal Bravais lattice [2]. The honeycomb structure in our experiment is induced by the intensity pattern $I(x, y)$ of three interfering plane waves, which is translated into a change in the refractive index Δn through the nonlinearity in a photorefractive crystal [15]. The paraxial evolution of ψ, the complex amplitude of a probe beam propagating in the lattice, is governed by the normalized Schrödinger-type equation [13,15]

$$i\frac{\partial\psi}{\partial z} + \nabla_\perp^2\psi - \frac{V_0\psi}{1 + I(x, y) + |\psi|^2} = 0. \qquad (1)$$

The potential depth and the nonlinearity are controlled by the parameter V_0. In our experiments on conical diffrac-

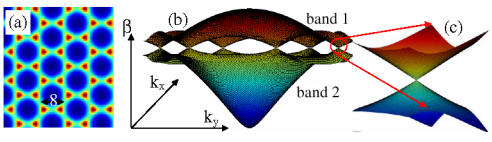

FIG. 1 (color online). The honeycomb lattice (a), and its band structure (b). Shown are bands 1,2, and the diabolical points where the bands intersect. Zooming in on one of these points reveals that dispersion is linear, in both bands, at the vicinity of a diabolic point (c).

tion, we use a low intensity probe beam [$|\psi|^2 \ll (1 + I)$] whose propagation is linear, whereas for solitons we use a high intensity probe propagating nonlinearly.

The band structure of this honeycomb lattice is calculated by solving the linear version of Eq. (1), yielding lattice modes $\psi = \exp(i\beta z)u(x, y)$. Equation (1) reduces to $\beta u = \nabla^2{}_\perp u + V(x, y)u$, yielding Bloch modes $u_k(x, y) = U_k(x, y)\exp(i\vec{k}_\perp \cdot \vec{r})$, where $\vec{k}_\perp = k_x\hat{x} + k_y\hat{y}$, and $U_k(x, y)$ has the lattice periodicity. The first two bands are shown in Fig. 1(b), resembling the band structure of graphene (with opposite sign), displaying six diabolic points [Figs. 1(b) and 1(c)]. These points arise from the honeycomb symmetry, irrespective of the details of each potential point or its depth, in a sharp contrast to other structures, where the existence of a gap between bands 1 and 2 depends on the potential depth (e.g., the square backbone lattice described in [15]). The diabolical points reside at the corners of the first Brillouin zone [Fig. 1(c)]. The dispersion relation at the vicinity of these points is conical: β in that region varies linearly with distance from the diabolic point. This is a characteristic feature of the intersection between two cones, which is what gives rise to diabolic points [1].

We first study wave propagation in the honeycomb lattice numerically (Fig. 2), by launching a beam with the structure of a Bloch mode associated with the diabolical point, multiplied by a Gaussian envelope. The Bloch modes at the tip can be constructed from pairs of plane waves with k vectors of opposite pairs of diabolical points. Thus, interfering two (or 4, or 6) plane-waves at angles associated with opposite diabolical points yields the phase structure of the modes from these points. Multiplying these waves by an envelope yields a superposition of Bloch modes in a region around these points.

Figure 2 shows an example of the propagation of a beam constructed to excite a Gaussian superposition of Bloch modes around a diabolic point. The input beam has a bell-shape structure, which, after some distance, transforms into the ring characteristic of conical diffraction. From there on, that ring is propagating with a constant thickness, while its radius is increasing linearly with distance. The invariance of the ring thickness manifests the linear dispersion relation above and below the diabolic points [Fig. 1(c)]; hence, the diffraction coefficient for wave packets constructed from Bloch modes in that region is zero (infinite effective mass). This is especially interesting because the ring itself is a manifestation of the dispersion properties at the diabolic point itself, where the diffraction coefficient is infinite (zero-effective mass). As a result, the ring forms a light cone in the lattice. In Fig. 2, the half-angle of the light cone is 20° in dimensionless units, matching the linear slope of the diffraction surface around the diabolical points. Translating Fig. 2 to dimensional units, for 500 nm wavelength, 10 μm lattice spacing, and 10^{-3} maximum index contrast, the light cone has half-angle of 0.34°.

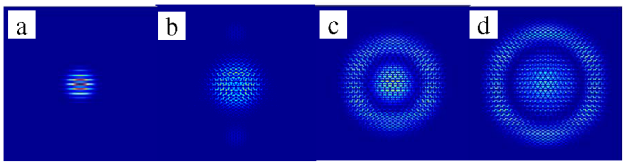

FIG. 2 (color online). Simulated propagation of a Gaussian superposition of Bloch modes associated with the vicinity of a diabolical point in a honeycomb lattice. Shown is the beam intensity at normalized propagation distances of 0, 50, 150, 200 (a)–(d). The input bell-shaped beam transforms into a ring of light of a nonvarying thickness, with a central spot.

The example of Fig. 2 was chosen because it is experimentally accessible. However, that input field excites not only Bloch modes near the diabolic points, but also of higher bands which do not display band crossing at the excitation momentum. As such, the light coupled to higher bands exhibits "conventional" diffraction broadening, giving rise to the central spot shown in Figs. 2(c) and 2(d). Zooming in on the central spot reveals that the intensity maxima reside between lattice sites, thus confirming that the spot originates from bands 3 and higher, in contrast to the ring, whose intensity maxima are on lattice sites, as expected from Bloch modes from the 1st and 2nd bands. The honeycomb lattice can therefore differentiate between light associated with bands 1 and 2, which diffracts conically into the outer ring, and light associated with bands 3 and higher, which remains in a central spot. It is also instructive to compare the conical diffraction in the honeycomb lattice to that occurring in a triangular lattice with the same spacing and potential depth. The unit cell of the triangular lattice is identical to that of the honeycomb, but with a central site; hence, the Brillouin zone edges are the same for both. We therefore launch the beam of Fig. 2(a) into the triangular lattice of the same parameters and simulate its propagation. Initially, a weak ring forms around a central spot, but this ring broadens and vanishes rapidly, with most of the power always in the central spot. The direct comparison between the two lattices under the same conditions confirms that conical diffraction is a characteristic feature associated with band crossing.

It is possible to gain insight into the quantitative features of conical diffraction in periodic structures by considering the following simplified model. Knowing the diffraction relation of the Bloch modes, we can formulate the propagation as a superposition of modes accumulating phases

$$\varphi(x, y, z) = \iint dk_x dk_y \Phi_0(k_x, k_y) e^{i\alpha z\sqrt{k_x^2+k_y^2}} U_{\vec{k}}(x, y) e^{i\vec{k}_\perp \cdot \vec{r}},$$

where $\varphi(x, y, z)$ is the optical field, and $\Phi_0(k_x, k_y)$ is the amplitude of the projection of the input field (at $z = 0$) on the Bloch modes $U_{\vec{k}}(x, y)e^{i\vec{k}_\perp \cdot \vec{r}}$. The phase term represents the conical diffraction relation around the diabolical point, where $\beta = \alpha\sqrt{k_x^2 + k_y^2}$ depends linearly on $|\vec{k}_\perp|$. Launching a beam with initial distribution $\Phi_0(k_x, k_y)$ of Bloch modes that is symmetric around the diabolical point, and changing integration variables so that $k_\perp = 0$ matches the diabolical point, yields

$$\varphi(x, y, z) = \int_0^\infty d\eta \eta \Phi_0(\eta) e^{i\alpha z \eta} \int_0^{2\pi} d\phi U_{\vec{k}}(x, y) e^{i\vec{k}_\perp \cdot \vec{r}}, \quad (2)$$

where $\eta = \sqrt{k_x^2 + k_y^2}$, $\tan\phi = k_y/k_x$. Because of the structure of the Bloch modes, this integral does not yield closed form solutions. However, for a sufficiently narrow distribution of Bloch modes, the wave functions $U_{\vec{k}}(x, y)$ vary only slightly for different k's, and thus can be approximated as having the same amplitude $U_{\vec{k}_d}(x, y)$ where $\vec{k}_d$ corresponds to the diabolical point. This approximation allows taking $U_{\vec{k}}(x, y)$ outside the integral, and the second integral in Eq. (2) gives the zero-order Bessel function, $J_0(\rho)$, where $\rho = \sqrt{x^2 + y^2}$. It is now possible to calculate the remaining integral numerically for any $\Phi_0(k_x, k_y)$. One example is the Gaussian distribution $\Phi_0(\eta) = e^{-g^2 \cdot \eta^2/2}$ used in the simulations of Fig. 2, but this does not yield a closed-form solution. Instead, using an exponential distribution, $\Phi_0(\eta) = e^{-g\eta}$, facilitates a closed-form solution

$$\varphi(\rho, \alpha z) = \frac{g - i\alpha z}{[(g - i\alpha z)^2 + \rho^2]^{3/2}}, \quad (3)$$

which encompasses the main features of the conical diffraction process in such lattices. Comparing the numerical solution of the integral in Eq. (2) with a Gaussian distribution, to the solution for an exponential distribution given by Eq. (3), reveals only minor differences. Hence, both initial distributions (as well as almost any initial bell-shaped distribution) evolve in the same fashion. It is therefore legitimate to relate the closed-form solution for the exponential distribution to the simulations and the experiments, which are both done with a Gaussian distribution. At $z = 0$, the solution [Eq. (3)] resembles a Lorentzian, which slowly transforms into a ring of light, whose radius expands with z while its thickness remains unchanged. Both the analytic model and the simulations (Fig. 2) display conical diffraction: a localized input beam with its Bloch mode distribution localized around a diabolic point transforms into a ring of light. Once the ring is formed (at $\alpha z \gg \rho$) it propagates with constant width, and the cone angle in both cases coincides with the angle extracted from the slope in the band structure to within 2.5% error.

Experimentally, we use the optical induction technique [12–14] to induce a honeycomb lattice on a photorefractive SBN:75 crystal. Our crystal is of dimensions of $2 \times 5 \times 10$ mm, where the extraordinary axis, along which the bias field ($\sim$1.5 kV/cm) is applied, is in the 2 mm direction, and the propagation axis is 10 mm long. The lattice was induced by the interference pattern of three broad beams ("plane waves"), with their k-vector projections on the transverse direction forming an equilateral triangle. These lattice-forming waves are at 488 nm wavelength, each with a intensity of $\sim$15 mW/cm^2, and they are ordinarily polarized so that they propagate linearly in the crystal, thereby creating a z-invariant photonic lattice [12,13]. To form the honeycomb lattice, we apply a negative bias field (field opposite to the direction of the extraordinary axis), thus using the self-defocusing nonlinearity to induce the lattice [15]. The resultant honeycomb lattice is depicted in Fig. 1(a), with an 8 μm distance between nearest neighbors. The probe beam entering the lattice is constructed from two 532 nm wavelength Gaussian beams, each with a 50 μm FWHM. The intensity of the probe beam is significantly lower than that of the lattice beams (by at least factor 10). The launch angles of the two Gaussian beams comprising the probe are aligned to match the diabolical points, thereby creating the intensity pattern of Fig. 3(a). The intensity pattern at the lattice output displays a ring of light with a dark spot at the center [Fig. 3(b)]. That is, the bell-shaped input beam evolves into a ring of light, thereby exhibiting conical diffraction. This conical diffraction approximately matches the simulation at dimensionless distance of 80, which corresponds to our $\sim$10 mm experimental propagation distance. Moreover, the angle of conical diffraction measured in our experiments is $\sim$0.34°, matching our simulations and analytic model to within 10%. Finally, when we turn the lattice off, the input beam diffracts in the homogeneous medium into the two-lobe beam shown in Fig. 3(c), proving that the ring of Fig. 3(b) results solely from diffraction in the honeycomb potential.

We now study spatial gap solitons [13,14,16–19] in honeycomb lattices [20]. Since honeycomb lattices have no complete gap between the 1st and the 2nd bands, for any potential depth, the first gap soliton appears in the gap between the 2nd and 3rd bands. Unlike rectangular or triangular lattices which possess only one atom per unit cell, the honeycomb lattice can only be described as a lattice with two atoms per unit cell. Consequently, both 1st and 2nd bands of the honeycomb lattice arise only from bound states (of the individual potential of one lattice site). Thus, the Bloch modes associated with the first two bands always have their intensity maxima located on lattice sites. This property is unique to honeycomb lattices; in other lattices, when V_0 is small, Bloch modes associated with band-2 (and higher) arise from unbound states of the individual potential. Consequently, the intensity peaks of 2nd-band Bloch modes in honeycomb lattices are always located on lattice sites. This feature of honeycomb lattices gives rise to spatial gap solitons located in the gap between band-2 and band-3, with the intensity maxima all located on lattice sites, but with a relative phase of π between

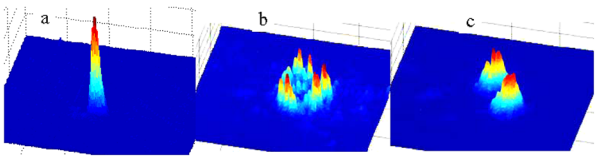

FIG. 3 (color online). Experimental results displaying (a) the bell-shaped input beam, (b) the conical diffraction ring exiting the honeycomb lattice, and (c) the far-field diffraction pattern of the beam when the lattice is "off."

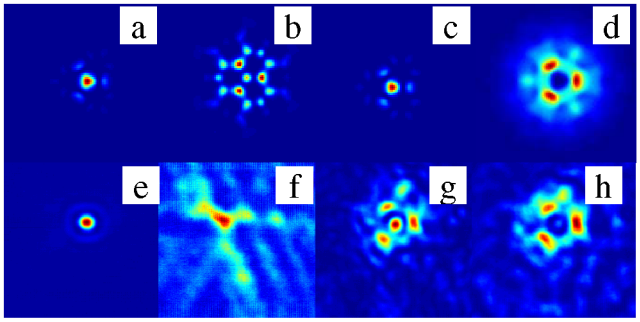

FIG. 4 (color online). (a)–(d) Simulation and (e)–(h) experiments with a "honeycomb gap soliton." (a),(e): (a) Calculated intensity structure of the soliton vs (e) experimental input beam. (b),(f): Intensity of the beam exiting the lattice, after linear diffraction in the lattice for $z = 30$ [units of Eq. (1)], and after propagating 10 mm in the experiment. (c),(g) Calculated and measured output intensity of the gap soliton. (d),(h) Calculated and measured phase structure of the soliton visualized by interference with a broad beam.

nearest-neighbor peaks. Such gap solitons are a manifestation of the special honeycomb symmetry, giving rise to two bands, both arising solely from bounded states.

We find spatial gap solitons with the self-consistency method [18]. Their wave functions arise from Bloch modes associated with the bottom of band 2. The intensity maxima have one central peak and three satellite lobes [Fig. 4(a)], with a π phase difference between the central peak and the three satellites [Fig. 4(d)]. We simulate the propagation of this wave packet numerically. In the linear regime, the input beam expands [Fig. 4(b)], undergoing anomalous diffraction, as expected from the dispersion curvature at the bottom of band 2. Thus, to form a spatial gap soliton from this wave packet, the nonlinearity must be of the self-defocusing type. At the proper (high) intensity, the self-defocusing nonlinearity balances the anomalous diffraction, forming a second-gap lattice soliton [Fig. 4(c)].

Our experiments on gap solitons are carried out in a honeycomb lattice with a nearest-neighbor spacing of 12 μm, under a bias field of -1000 V/cm. The 532 nm probe beam has a central peak and an outer ring, with a relative phase of π, which is close to the structure of the soliton. We construct such a beam from the far-field diffraction pattern of a circular aperture, which is a Bessel-beam with the proper phase relation. The intensity of the input beam [Fig. 4(e)] displays a main lobe filling one lattice site, and the first order of the Bessel beam (the ring) adjusted to match the nearest-neighbor sites. Figure 4(f) displays the output intensity under linear conditions (very low intensity), revealing a tripodlike diffraction in the lattice. At peak intensity ~ 10 Watt/cm^2, the beam evolves into a soliton [Fig. 4(g)]. The phase structure of the output soliton is revealed by interfering it with a weakly diverging Gaussian beam. When the central lobe of the soliton interferes destructively with the Gaussian beam, the three satellites interfere with it constructively [Fig. 4(h)]. Thus, the central lobe and the three satellites have a relative phase of π. We therefore conclude that the input beam has evolved into a tripod-shaped beam [Fig. 4(g)] with the proper phase structure [Fig. 4(h)] of a spatial gap soliton arising from the base of the second band of a honeycomb lattice.

In conclusion, we studied waves in honeycomb photonic lattices, demonstrating the first observation of conical diffraction arising solely from the periodicity of the potential, and of spatial "honeycomb gap solitons." These ideas raise several intriguing questions. For example, it is possible to observe Pogendorf's dark ring [1] arising from conical diffraction in a periodic lattice? How does nonlinearity affect conical diffraction? Are there any other periodic structures possessing diabolic points? These intriguing questions are universal, and relate to any field in which waves can propagate in a periodic potential.

[1] M. V. Berry and M. R. Jeffrey, Prog. Opt. (to be published).
[2] P. R. Wallace, Phys. Rev. **71**, 622 (1947).
[3] K. S. Novoselov *et al.*, Science **306**, 666 (2004); Nature (London) **438**, 197 (2005).
[4] Y. Kayanuma, Phys. Rev. A **55**, R2495 (1997).
[5] Chang-Soo Park *et al.*, Phys. Rev. B **65**, 064411 (2002).
[6] W. Domcke *et al.*, Mol. Phys. **43**, 851 (1981); see also *Conical Intersections*, edited by W. Domcke, D. R. Yarkony, and H. Koppel (World Scientific, Singapore, 2004).
[7] W. R. Hamilton, Trans. R. Irish Acad. **17**, 1 (1837).
[8] H. Lloyd, Trans. R. Irish Acad. **17**, 145 (1837).
[9] R. I. Egorov *et al.*, Opt. Lett. **31**, 2048 (2006).
[10] Note the fundamental difference between conical diffraction phenomena [1,7], which are inherently linear processes of diffraction, and conical emission accompanying nonlinear optical processes with noncollinear beams. See, e.g., D. Faccio *et al.*, Phys. Rev. Lett. **96**, 193901 (2006); E. Nibbering *et al.*, Opt. Lett. **21**, 62 (1996).
[11] To distinguish from periodic systems made up of materials displaying diabolic points, e.g., J. B. Harris *et al.*, J. Opt. Soc. Am. A **13**, 803 (1996).
[12] N. K. Efremidis *et al.*, Phys. Rev. E **66**, 046602 (2002).
[13] J. W. Fleischer *et al.*, Phys. Rev. Lett. **90**, 023902 (2003).
[14] J. W. Fleischer *et al.*, Nature (London) **422**, 147 (2003).
[15] N. K. Efremidis *et al.*, Phys. Rev. Lett. **91**, 213906 (2003).
[16] Y. S. Kivshar, Opt. Lett. **18**, 1147 (1993).
[17] D. Mandelik *et al.*, Phys. Rev. Lett. **92**, 093904 (2004); D. Neshev *et al.*, *ibid.* **93**, 083905 (2004).
[18] O. Manela *et al.*, Opt. Lett. **29**, 2049 (2004); G. Bartal *et al.*, Phys. Rev. Lett. **95**, 053904 (2005).
[19] D. N. Christodoulides *et al.*, Nature (London) **424**, 817 (2003).
[20] For solitons residing in the semi-infinite gap of a honeycomb lattice, see P. G. Kevrekidis *et al.*, Phys. Rev. E **66**, 016609 (2002).